

Parameter Identification and Model Reduction in the Design of Alkaline Methanol Fuel Cells

Tanja Clees^(1,2), Bernhard Klaassen⁽²⁾, Igor Nikitin⁽²⁾, Lialia Nikitina⁽²⁾, Sabine Pott⁽²⁾,
Ulrike Krewer⁽³⁾, Theresa Haisch^(3,4), Fabian Kubannek⁽³⁾

⁽¹⁾ University of Applied Sciences Bonn-Rhein-Sieg, Sankt Augustin, Germany

⁽²⁾ Fraunhofer Institute for Algorithms and Scientific Computing, Sankt Augustin, Germany

Email: Name.Surname@scai.fraunhofer.de

⁽³⁾ Institute of Energy and Process Systems Engineering, Technical University, Braunschweig, Germany

Email: {u.krewer, f.kubannek}@tu-braunschweig.de

⁽⁴⁾ DECHEMA Research Institute, Frankfurt am Main, Germany

Email: theresa.haisch@dechema.de

Abstract—Alkaline methanol oxidation is an important electrochemical process in the design of efficient fuel cells. Typically, a system of ordinary differential equations is used to model the kinetics of this process. The fitting of the parameters of the underlying mathematical model is performed on the basis of different types of experiments, characterizing the fuel cell. In this paper, we describe generic methods for creation of a mathematical model of electrochemical kinetics from a given reaction network, as well as for identification of parameters of this model. We also describe methods for model reduction, based on a combination of steady-state and dynamical descriptions of the process. The methods are tested on a range of experiments, including different concentrations of the reagents and different voltage range.

Keywords—*modeling of complex systems; observational data and simulations; advanced applications; mathematical chemistry.*

I. INTRODUCTION

This work extends our conference paper [1], where the methods for model reduction in electrochemical kinetics of alkaline methanol fuel cells have been introduced. Here we present more details on different types of experiments, characterizing the fuel cell behavior, as well as the methods for automatic generation of a mathematical model from chemical reaction description, the methods of parameter identification, and more testing results for these methods.

Galvanic cell is a chemical source of electric current based on interaction of two metals in electrolyte. Fuel cells are similar to galvanic cell but the reagents can be refilled multiple times. A special class of the fuel cells are direct fuel cells, in which formation of hydrogen is avoided, providing more safety for the usage. Renewable sources of energy are provided by alcohols, most commonly used are methanol and ethanol. In fuel cells, the chemical reaction of oxidation, the burning of the alcohols, is directly transferred to the electric energy.

The methods of parameter identification in electrochemical kinetics have been presented in our papers [2–4]. They include three types of experiments, measuring stationary state of the cell for a given voltage, small harmonic oscillations near this state and the response of the cell to a large amplitude variation of the voltage. The theoretical basis for these experiments can be found in the works [5–9]. Our purpose is the application of these general methods to a particular system, describing electrooxidation of the methanol in alkaline medium.

In Section II we describe the experiments, characterizing the fuel cell of alkaline methanol type. In Section III the methods of model generation and parameter identification are presented. Further improvements of the methods by model reduction and the results of their application to the experimental data are given in Section IV.

II. THE EXPERIMENT

The experimental setup is shown on Figure 1. It is efficiently designed to avoid external influence and minimize processes, which could violate the results of modeling. The cell itself (1) is made of teflon to provide maximal tightness of the parts. The working electrode (2) is a disk coated with a platinum catalyst. The disk is rapidly rotated to suppress diffusion effects. There is a counter electrode (3) made of a platinum wire and a reference electrode (4) made of Hg/HgO , used for recalculation of potentials. The temperature in the cell is measured by sensor (5). The forming and remaining environmental CO_2 is removed from the cell by permanent argon blow (6). The setup is put under deep vacuum. During the experiments, the voltage in the cell is set and the current is measured. Inbetween the experiments, high amplitude voltage variations are used for electrochemical cleaning of the electrode.

Three types of experiments are performed, see Figure 2. Polarization Curve (PC) represents the stationary state of the cell. For this purpose the voltage is changed very slowly in equidistant steps, on each step the stabilized current is measured. Electro-Impedance Spectrometry (EIS) probes the cell with harmonic oscillations of small amplitude in the vicinity of the stationary state, with the frequency varied in a large range. A linearized behavior of the system is characterized by complex-valued resistance, an impedance of the cell, which is computed and displayed on Nyquist plot diagrams. Cyclic Voltammetry (CV) probes the cell with a periodic saw-like voltage profile of high amplitude and measures the corresponding volt-ampere dynamical characteristics. The corresponding plot contains non-split stationary PC-part and a hysteresis loop, representing non-stationary, dynamical effects.

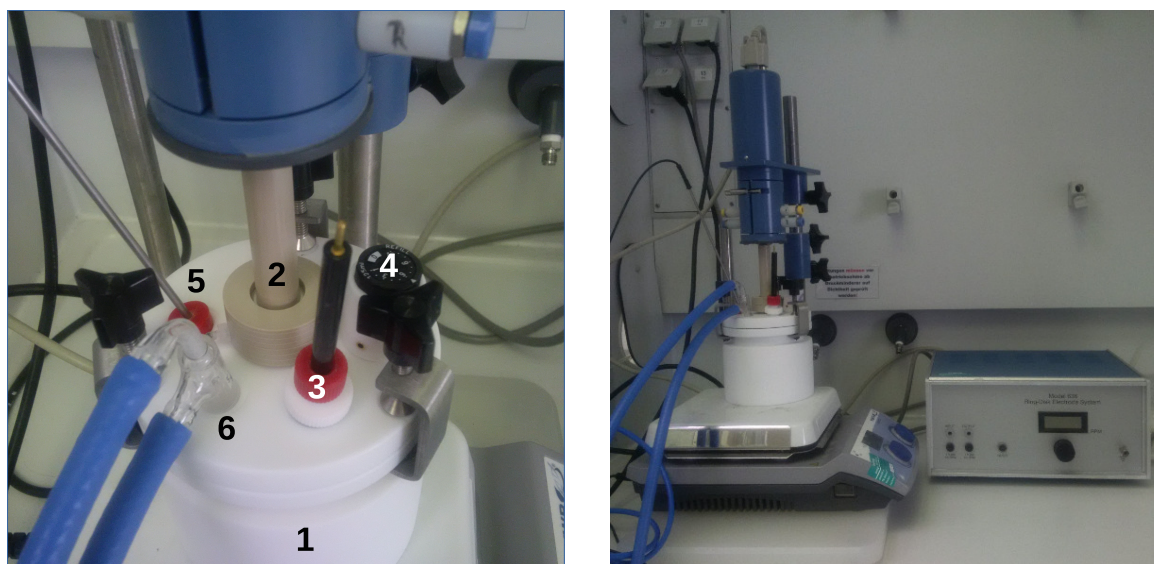


Figure 1. On the left: the experimental setup, consisting of a teflon cell (1) under deep vacuum, the rotating working electrode (2), the counter electrode (3), the reference electrode (4), the temperature sensor (5) and argon blow supply (6). On the right: a general view with service equipment.

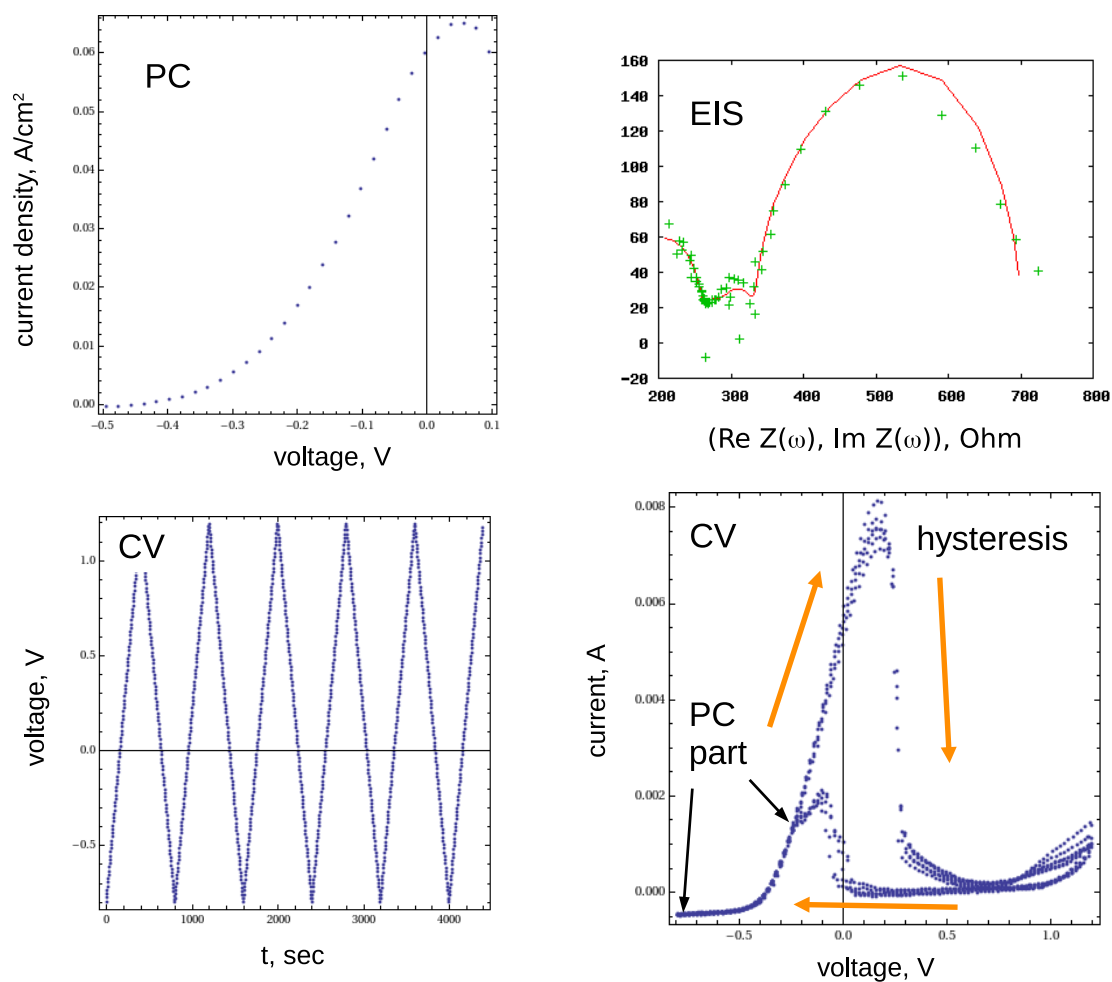


Figure 2. Three types of experiments (PC, EIS, CV), characterizing the cell.

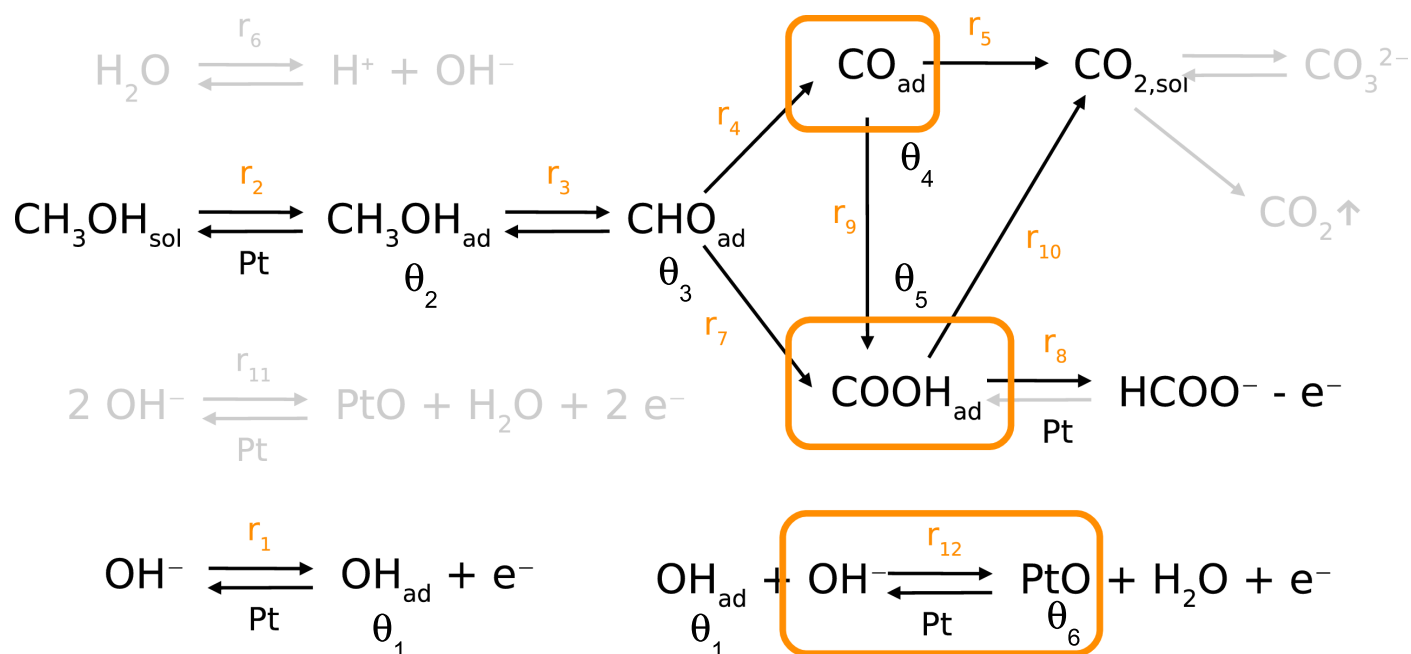


Figure 3. The chemical reactions network, the orange boxes show the reactions potentially responsible for the hysteresis effect on the CV plot.

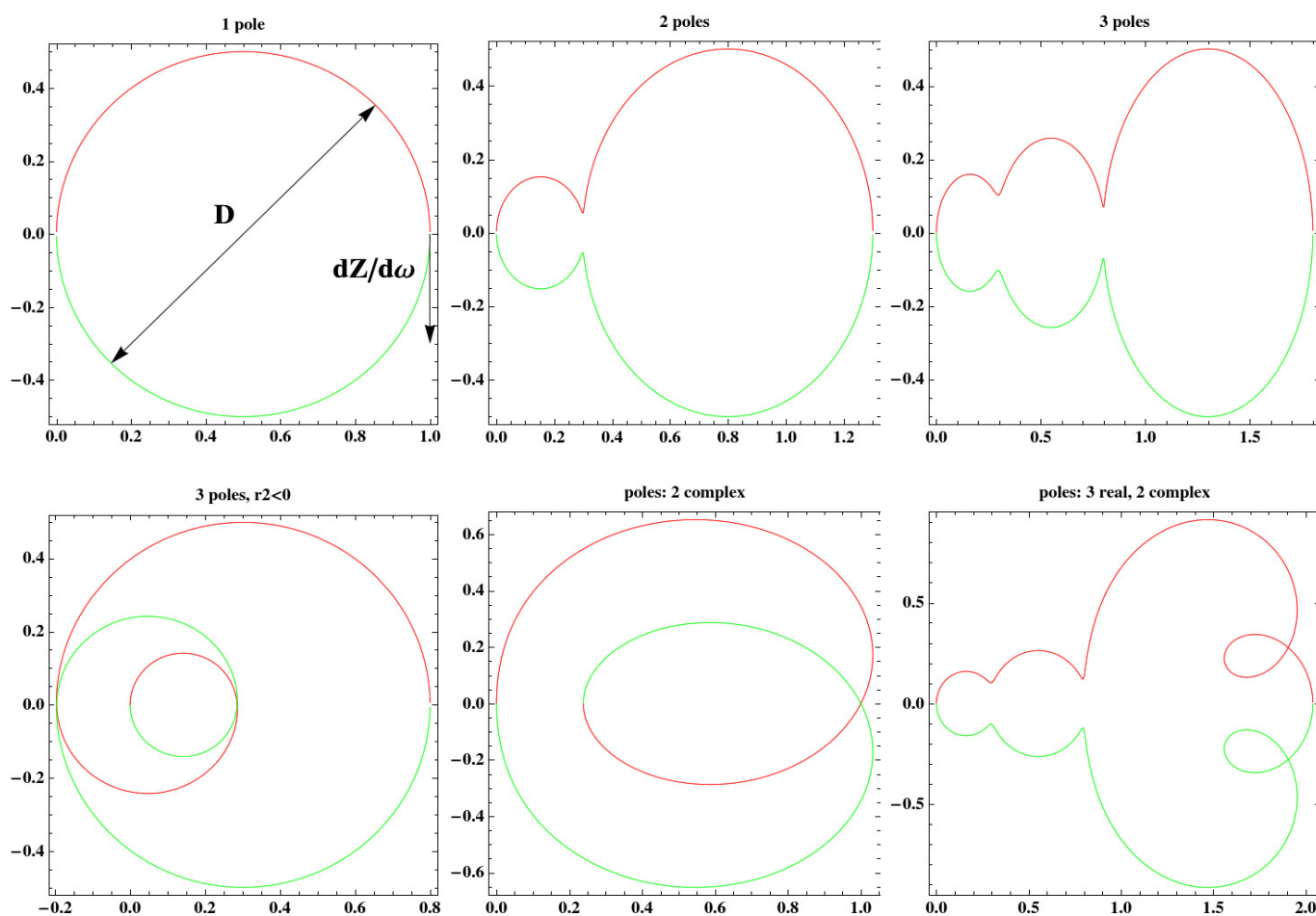


Figure 4. Typical shapes of EIS diagrams. Image from [4].

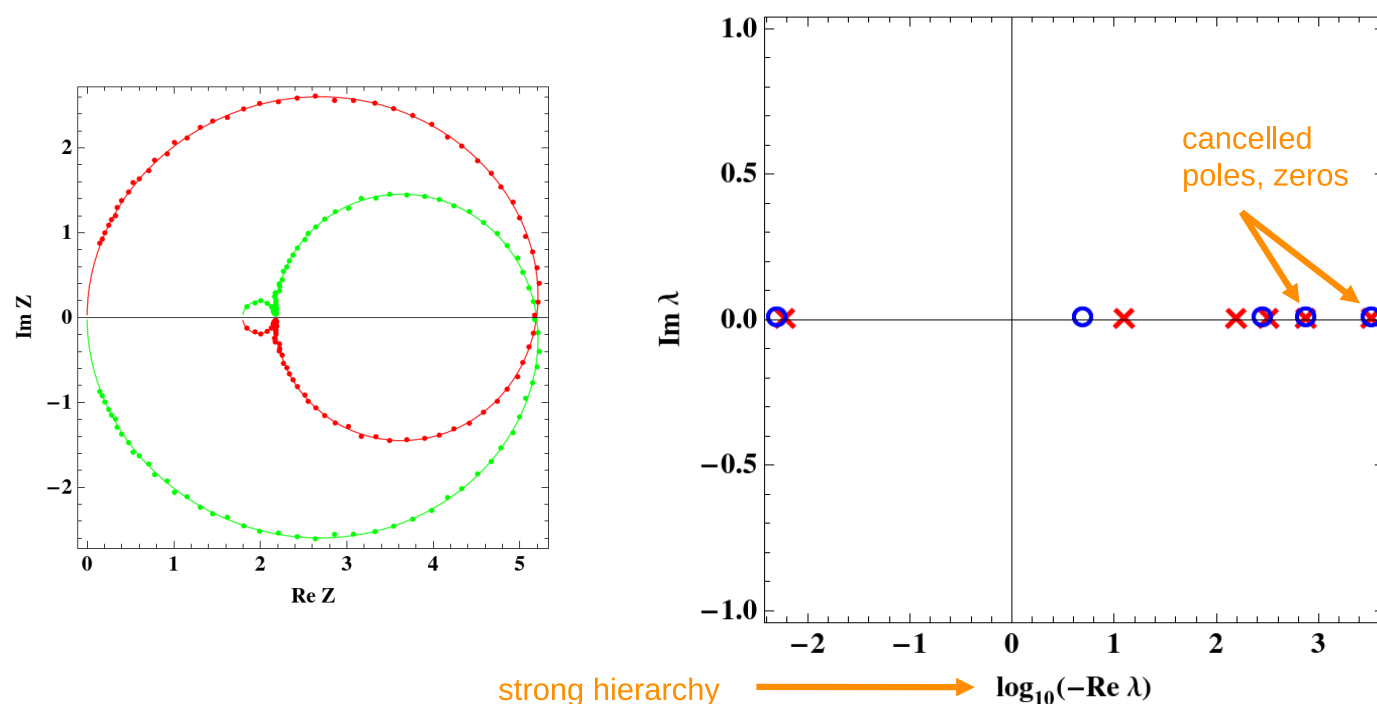


Figure 5. Nyquist plot (on the left) and reconstructed poles and zeros (on the right). Image from [4].

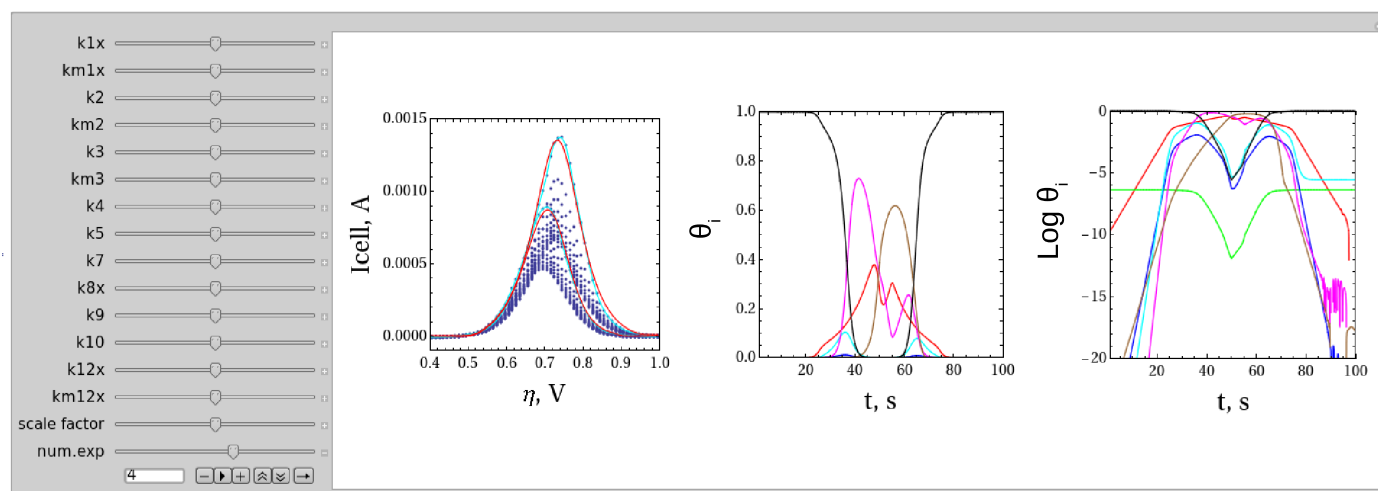


Figure 6. Interactive tool for parameter space exploration (in Mathematica v11).

III. THE MODEL

The chemistry of the cell is described by the network of reactions, shown on Figure 3 and Table I. It includes the chain of the oxidation of carbon containing reagents, starting from methanol CH_3OH in the solution (subscript *sol*) and up to carbon dioxide CO_2 , finally removed from the system. In parallel, the process of transformation of hydroxyl ion OH^- is present. All processes start from adsorption of fuel and hydroxyl on the platinum catalyst (subscript *ad*). Some of the reactions are reversible, so that the direct and reverse chemical processes are shown by two oppositely directed arrows. Our previous investigation [3] allows to exclude some originally

postulated reactions from the model, due to their vanishingly small influence on the result. On Figure 3, these reactions are grayed out and in the mathematical model they can be omitted by setting the corresponding reaction constants to zero. Also in our study [2], [3] we have identified reactions, related with weakly coupled intermediates, which could serve as a source for the hysteresis and other dynamical effects. On the reaction scheme, they are highlighted by orange bubbles. Most of important among them is a reaction r_{12} , describing formation of platinum monoxide PtO .

Proceeding to the mathematical description of electrochemical kinetics, we note that the reaction network on Figure 3

can be represented as a *hypergraph*, a generalization of graph where an edge can join any number of vertices. It can be described by an incidence matrix a_{ij} , for ending vertices (j) entering in an edge (i). We use an approach, initially developed for transport network problems in our paper [10], where the mathematical modeling of network problems can be represented as a *translation* between two domain specific languages (DSL1,2). One is a network description language (NET), used in the corresponding discipline (e.g., electrochemistry, gas transport, water supply, etc.), another one is a problem description language (PRO), understood by generic non-linear solvers (e.g., IPOPT, Mathematica, Matlab, etc.). The generic algorithm (Universal Translation, UT) uses a configurable set of translation rules (Translation Matrix, TM) for translating the network from one representation to another:

$$NET \times TM \rightarrow PRO. \quad (1)$$

In application to chemical kinetics, the reaction hypergraph from Table I is recorded in a symbolic form (NET):

$$\text{reaction}_i = \sum_j a_{ij}^L g_j - a_{ij}^R g_j, \quad (2)$$

where g_j are the reagents (e.g., OH^- , CH_3OH), a_{ij}^L , a_{ij}^R are the incidence matrices of the hypergraph multiplied to *stoichiometric coefficients*. These integer-valued coefficients indicate how many molecules are spent or produced, for the left and right hand side of the reaction. The translation matrix (TM) defines the rules of translation, enlisting the reagents, variables, constants, parameters, an excerpt is shown in Table II. The hypergraph is then translated to the reaction rates

$$r_i = k_i^L \prod_j (c_j)^{a_{ij}^L} - k_i^R \prod_j (c_j)^{a_{ij}^R}, \quad (3)$$

indicating how many reactions per second are happening. The rates are defined by a *probability* of the reagents to meet each other for the reaction, proportional to the product of concentrations c_j (that can be molar, volumetric, surface, etc.), in the corresponding integer powers. E.g., the reaction r_5 in Table I requires one molecule CO_{ad} (reagent 4, see Table II) to meet two molecules of OH_{ad} (reagent 1), and the corresponding reaction rate will be proportional to $c_4 c_1^2$. The proportionality coefficients k_i are important model parameters, which should be reconstructed from the experiments. Further, the reaction rates are assembled to molar balance description:

$$F_j = - \sum_i r_i (a_{ij}^L - a_{ij}^R), \quad (4)$$

indicating how many molecules (or, in appropriate normalization, moles) of the reagents are spent or produced per second. Then ordinary differential equations (ODEs) governing the chemical kinetics are formed:

$$d\nu_i/dt = F_i, \quad (5)$$

where ν_i is a molar amount for the i -th reagent.

In particular applications, these generic formulae can be modified by different normalizations, e.g., some of the reagents can be adsorbed on the electrode and are represented by dimensionless surface coverage ratios, with the range $\theta_i \in [0, 1]$. Also, a peculiarity of electrochemistry is that the electrons also

belong to the reagents and their flow (electrons per second) defines the cell current measured in the experiments.

Applying these translation rules to our reaction network, we obtain [3]:

$$\begin{aligned} r_1 &= k_1 c_1 \theta_0 - k_{-1} \theta_1, \\ r_2 &= k_2 c_2 \theta_0 - k_{-2} \theta_2, \\ r_3 &= k_3 \theta_2 \theta_1^3 - k_{-3} \theta_3 c_3^3, \\ r_4 &= k_4 \theta_3 \theta_1, \quad r_5 = k_5 \theta_4 \theta_1^2, \\ r_7 &= k_7 \theta_3 \theta_1^2, \quad r_8 = k_8 \theta_5, \\ r_9 &= k_9 \theta_4 \theta_1, \quad r_{10} = k_{10} \theta_5 \theta_1, \\ r_{12} &= k_{12} c_1 \theta_1 - k_{-12} c_3 \theta_6, \end{aligned} \quad (6)$$

where $\theta_0 = 1 - \sum_{i=1}^6 \theta_i$ is a part the surface of platinum catalyst, not covered by any reagent, $\theta_0 \in [0, 1]$. For the reactions, involving electrons, the Tafel equation is used:

$$\begin{aligned} k_1 &= k_1^0 \exp(\alpha \beta \eta), \\ k_{-1} &= k_{-1}^0 \exp(-(1 - \alpha) \beta \eta), \\ k_8 &= k_8^0 \exp(-(1 - \alpha) \beta \eta), \\ k_{12} &= k_{12}^0 \exp(\alpha \beta \eta), \\ k_{-12} &= k_{-12}^0 \exp(-(1 - \alpha) \beta \eta), \\ \beta &= F/(RT), \end{aligned} \quad (7)$$

where T is the absolute temperature and other constants are given in Table II,

$$\begin{aligned} F_1 &= (r_1 - 3r_3 - r_4 - 2r_5 - 2r_7 - r_9 - r_{10} - r_{12})/C_{act}, \\ F_2 &= (r_2 - r_3)/C_{act}, \\ F_3 &= (r_3 - r_4 - r_7)/C_{act}, \\ F_4 &= (r_4 - r_5 - r_9)/C_{act}, \\ F_5 &= (r_7 - r_8 + r_9 - r_{10})/C_{act}, \\ F_6 &= r_{12}/C_{act}, \\ F_7 &= (-r_1 + r_8 - r_{12}) \cdot FA/C_{dl}, \end{aligned} \quad (8)$$

here the constants C_{act} , C_{dl} , A are also given in Table II, these 3 constants depend on the experimental setup and recalibrated each time when it is changed. The resulting ODE system looks like:

$$\begin{aligned} d\theta_i/dt &= F_i(\theta, \eta), \quad i = 1 \dots 6, \\ d\eta/dt &= F_7(\theta, \eta) + I_{cell}/C_{dl}, \end{aligned} \quad (9)$$

where η is the cell voltage and I_{cell} is the cell current. The model is fitted to the experiment using L_2 -norm of variation

$$L_2 = \left(\sum_i (I_{cell,i} - I_{cell,i}^{exp})^2 \right)^{1/2}, \quad (10)$$

with the reaction constants $k_i^0 \geq 0$ in (7) and $k_i \geq 0$ for all others used as fitting parameters. The details of fitting depend on the selected experimental method.

PC method: sets all time derivatives to zero, to define a stationary point

$$\begin{aligned} 0 &= F_i(\theta^*, \eta^*), \quad i = 1 \dots 6, \\ 0 &= F_7(\theta^*, \eta^*) + I_{cell}^*/C_{dl}, \end{aligned} \quad (11)$$

for fixed η^* , stepwise scanned in the range $[\eta_{min}, \eta_{max}]$, the obtained 7×7 polynomial system is solved with respect to

TABLE I. The reaction list.

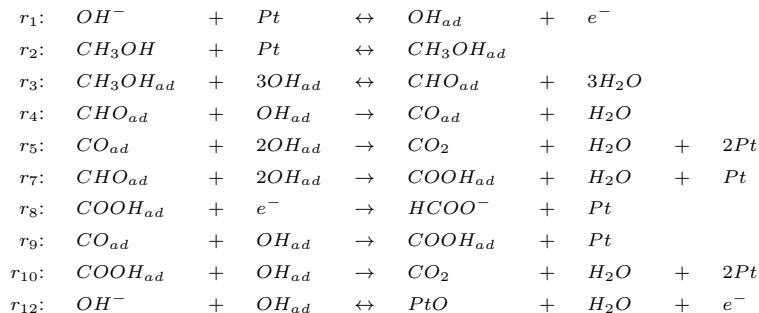


TABLE II. Numeration and values for the model variables and constants.

Variables	Concentrations	Constants	Names	Values
θ_1 OH_{ad}		F	Faraday constant	$9.649 \cdot 10^4$ C/mol
θ_2 CH_3OH_{ad}	c_1 OH^-	R	universal gas constant	8.314 J/(K mol)
θ_3 CHO_{ad}	c_2 CH_3OH	α	charge transfer coefficient	0.5
θ_4 CO_{ad}	c_3 H_2O	C_{dl}	capacitance	$1.899 \cdot 10^{-4}$ F
θ_5 $COOH_{ad}$		C_{act}	activity constant	$8.523 \cdot 10^{-5}$ mol/m ²
θ_6 PtO		A	electrode area	$2.376 \cdot 10^{-5}$ m ²

$(\theta_{1-6}^*, I_{cell}^*)$ by *Mathematica* NSolve algorithm. Only real roots with $\theta_{0-6}^* \in [0, 1]$ are selected. There are always 2 such roots, one is trivial: $\theta_4^* = 1$, other $\theta_i^* = 0$, $I_{cell}^* = 0$ (electrode is completely blocked by CO_{ad}), another is non-trivial: all $\theta_i^* > 0$, $I_{cell}^* > 0$. Only non-trivial root is selected and used for minimization of L_2 -norm (10).

EIS method: linearizes the system near the stationary point

$$dv/dt = Jv + b, \quad J_{ij} = \partial F_i / \partial x_j, \quad (12)$$

with $n \times n$ Jacobi matrix J , n -dimensional vector of variables $x = (\theta_1, \dots, \theta_{n-1}, \eta)^T$ (in our case $n = 7$) and variations of vectors $v = \delta x$, $b = (0, \dots, 0, \delta I_{cell} / C_{dl})^T$. In more details we have considered this system in our previous paper [4]. The equations describe the linearized evolution around the stationary point, when the voltage is varied along the given profile. In our case, harmonic oscillations of small amplitude are considered, in complex denotation: $\delta \eta = \eta_0 \exp(i\omega t)$, $\delta I_{cell} = I_0 \exp(i\omega t)$. Their ratio gives the complex resistance, or impedance $Z = \eta_0 / I_0$ of the cell. After harmonic substitution $v = v_0 \exp(i\omega t)$, $b = b_0 \exp(i\omega t)$ we have

$$(i\omega - J)v_0 = b_0 \quad (13)$$

and finally

$$C_{dl}Z(\omega) = ((i\omega - J)^{-1})_{nn}. \quad (14)$$

It can be rewritten in one of the equivalent forms:

$$C_{dl}Z(\omega) = Q_{n-1}(i\omega) / Q_n(i\omega), \quad (15)$$

where Q_k are polynomials of k -th order,

$$C_{dl}Z(\omega) = \prod_{j=1}^{n-1} (i\omega - q_j) / \prod_{j=1}^n (i\omega - p_j), \quad (16)$$

with poles p_j and zeros q_j of Z ,

$$C_{dl}Z(\omega) = \sum_{j=1}^n r_j / (i\omega - p_j), \quad (17)$$

with residues r_j at the corresponding poles p_j . Note that p_j are eigenvalues of Jacobi matrix J , while q_j are eigenvalues of its left-upper $(n-1) \times (n-1)$ submatrix.

The fitting involves a solution of Non-Linear Program (NLP) of the form

$$\text{find } \min_x f(x), \text{ such that } g(x) = 0 \text{ and } h(x) \geq 0, \quad (18)$$

where the equality conditions g include the equations for stationary point (11), the definition of Jacobi matrix in (12) and the definition of poles and zeros

$$Q_{n-1}(q_j) = 0, \quad Q_n(p_j) = 0, \quad (19)$$

the inequality conditions h include the already mentioned

$$k_r \geq 0, \quad \theta_i^* \geq 0, \quad \theta_0^* = 1 - \sum \theta_i^* \geq 0. \quad (20)$$

In the case, if the obtained system becomes overdetermined, some of the equations can be moved to the target function, e.g.,

$$f(x) : L_2 = \sum_j |Q_{n-1}(q_j)|^2 + \sum_j |Q_n(p_j)|^2. \quad (21)$$

The solution is performed by *Mathematica* NMinimize algorithm. The typical model shapes on the Nyquist plot corresponding to a different number and types of poles and zeros are shown on Figure 4. One of these forms has been used on Figure 5 for testing of the reconstruction algorithm. The paper [4] provides further details on the structure of solution. In particular, if some poles and zeros come too close to each other, they should be mutually cancelled to increase stability of the reconstruction. The stability condition has a

form $N_{exp}(N_p + N_z + 1) \geq N_k$, where N_{exp} is the number of experiments, $N_{p,z}$ is the number of reconstructed poles and zeros per experiment, N_k is the number of reaction constants. The errors of the reconstructed Nyquist plot can be controlled by the formula

$$\delta Z(\omega)/Z(\omega) = -\sum \delta q_j/(i\omega - q_j) + \sum \delta p_j/(i\omega - p_j). \quad (22)$$

CV method: considers the original ODE system (9). We solve this system directly via numerical integration by *Mathematica* `NDSolve` algorithm. The starting point of the integration should be selected to provide cyclicity of solution $\theta(T_p) = \theta(0)$, T_p is a period. Alternatively, the system should be integrated during several (3-5) “warming up” periods till the cycle becomes reproduced. The resulting I_{cell} is used for fitting of L_2 -norm (10) by *Mathematica* `NMinimize` algorithm. The main problem is a determination of a region in multi-dimensional ($dim = 14$ in our case) space of the fitting parameters, the reaction coefficients $k_i^{(0)}$, where the starting point for fitting procedure is located, close enough to the minimum searched. We solved this problem in [2] by an iterative direct search Monte Carlo method in a combination with interactive visualization. Figure 6 shows the visualization tool, implemented by means of *Mathematica* `Manipulate` algorithm. The user can interactively change the reaction constants and see the obtained integrated evolution in comparison with the experimental data.

The first interesting observation, obtained by the described method, is that CV diagrams at low voltages contain a PC part, where the shapes for increasing and decreasing voltage coincide and the time derivatives in (9) can be omitted. These parts, displayed on Figure 7 for the experiments with different volumetric concentrations of the reagents, can be fitted by the stationary curves from the above described PC method. Although this method does not require computationally expensive numerical integration and is very fast, its disadvantage is that only the ratios of reaction coefficients can be reconstructed. Indeed, for the absent time derivatives in (11), every equation can be divided to one of the reaction constants, preserving its validity.

At larger voltages, a hysteresis effect appears, see Figure 8. It is purely dynamic effect, related with the presence of time derivative in (9), which after time-reflection reverses its sign. As a result, the shapes of volt-ampere characteristics for increasing and decreasing voltage do not coincide. Our analysis in [2], [3] shows that the hysteresis effect appears when some intermediates in the reaction network are weakly coupled. In this case the corresponding θ evolution becomes retarded with respect to the voltage variation. We have tried to decouple several intermediates, indicated by orange bubbles in Figure 3, by strongly reducing their reaction constants. The best results are obtained with decoupling of the 6th reagent, *PtO*.

Next, Figure 9 shows CV plots in experiments with different upper voltage η_{max} . The data are described in details in [12], where the focus is on the physical-chemical processes, while in the current paper we focus on the simulation methodology and the parameter identification of the mathematical model. It is visible in Figure 9, how hysteresis is reduced and finally disappears, leaving PC behavior only, when η_{max} is decreasing. Again, the hysteresis effect vanishes when η_{max}

is shifted below the voltage region, where the production of *PtO* happens. Therefore, the PC and EIS methods should be preferably applied in this low voltage region.

The experimental data on Figures 7 and 8 are well fitted by the model. This fit is performed individually for every plot, presenting given values of concentrations, as described in [3]. An attempt to fit all experiments by a single set of reaction constants fails, which has been interpreted in [3] as a dependence of reaction constants on concentrations.

The experimental data on Figure 9 correspond to the same concentration values and variable η_{max} . Three columns correspond to three isolated optima of the fit, presented on Figure 10. The best fit is provided by the left column, set 1. It is visible that the upper increasing curve always has a better fit than the lower decreasing one. It is also visible that the shape of the increasing curve is the same for all experiments, only the upper limit is different. This happens because we are fitting the first cycle of CV plot. Comparing the plots in different rows, we can conclude that the system initially “does not know”, when its η will be reverted, and produces the same curve upto this moment. We also observe that the decreasing curve is sensitive to the small values of θ_0 in the region of upper voltage and fluctuates when the model parameters are slightly changed. More uncertainty is related with the unknown starting θ -values for the evolution on the first cycle, for which in our experiments the clean electrode $\theta_0 = 1$ was assumed. There is also a large visible scatter in the data, corresponding to different cycles of the CV plot. Like it happens with slow approaching of the equilibrium in PC experiments, here we observe a slow approaching of the limit cycle in CV plots.

IV. IMPROVEMENTS OF CV METHOD

In this section, we consider a possibility that the ODE system (9) can be reduced to the system of Differential-Algebraic Equations (DAE), where some of the equations keep time derivative terms and the others do not. Let us write the equations in the form:

$$\alpha_i d\theta_i/dt = F_i = \sum_j C_{ij} r_j, \quad (23)$$

where C_{ij} is a structural matrix relating production rates F_i and reaction rates r_j and α_i are constant coefficients, for the case of ODE set to $\alpha_i = 1$ and for the case of DAE to $\alpha_i = 0$. We have also reassigned normalization factors between F_i and r_j , so that both are measured in the same units (s^{-1}). The measured quantity is a cell current, given by the expression:

$$I_{cell} = FAC_{act} F_7, \quad F_7 = \sum_j C_{7j} r_j. \quad (24)$$

Here, we add the 7th row in the structural matrix and omit the practically vanishing capacitance term $C_{dl} d\eta/dt$.

Now, we draw attention to Figure 11, which depicts the evolution of production and reaction rates. It is visible that some r_j compensate each other, resulting in almost zero F_i . This common property, also noted in [11], means that some of the reactions proceed so fast that they are almost permanently in equilibrium. One production rate is not in equilibrium. It is also characterized by the presence of only one reaction: $F_6 = r_{12}$. Thus, in the equations, one can switch off the dynamic terms for all reagents except for the 6th, so that $\alpha_i = \delta_{i6}$. As a result, the ODE system is replaced by an equivalent DAE system. *Mathematica* v11 can be used to solve DAE systems with the same efficiency as ODE.

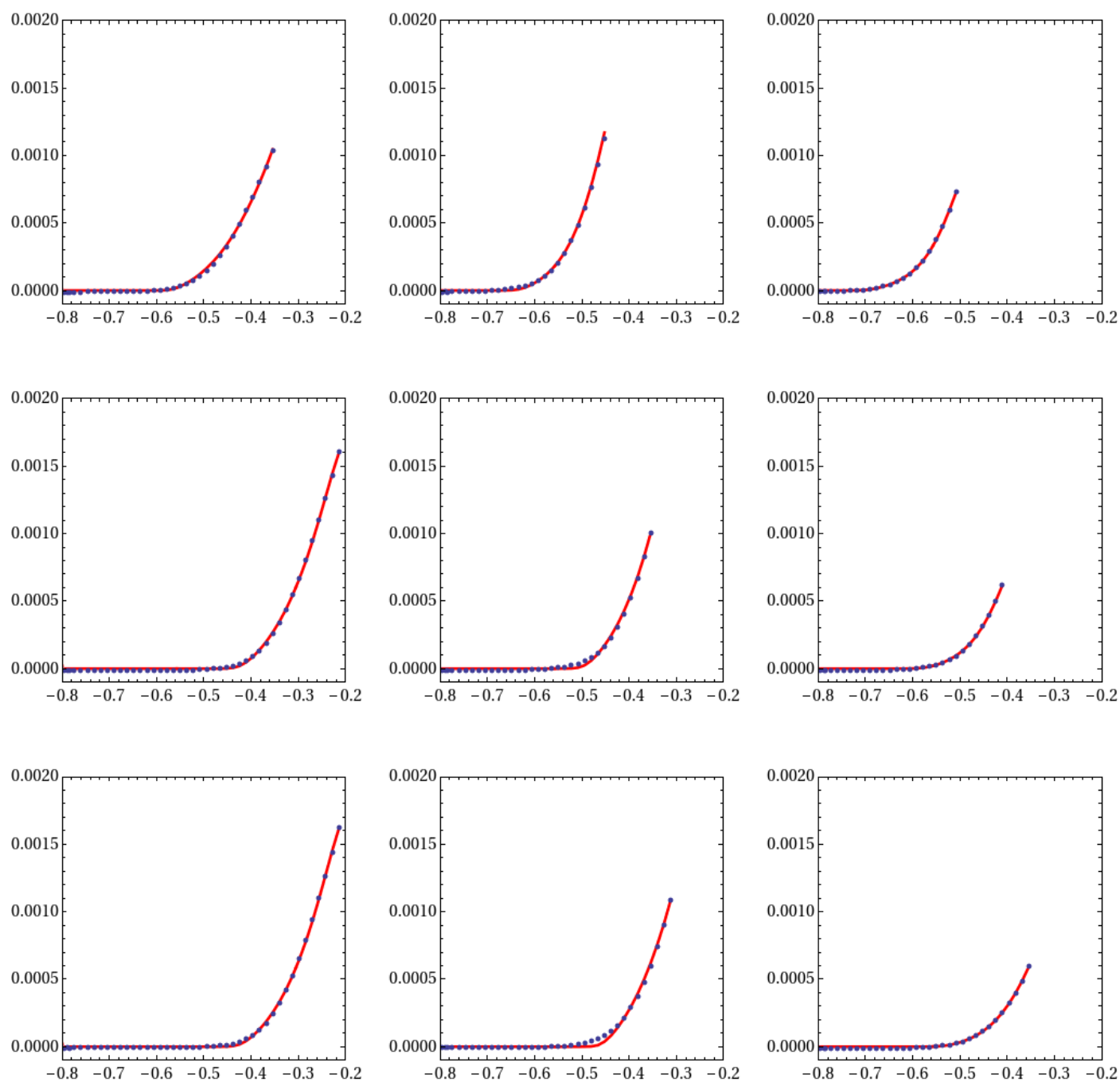


Figure 7. PC experiments. From left to right, the concentration of alkaline KOH is set to $c_1 = \{0.1, 0.5, 1.0\}M$, from bottom to top, the concentration of methanol CH_3OH is set to $c_2 = \{0.5, 0.75, 1.0\}M$. Horizontal axes represent the voltage in Volts, vertical axes – the cell current in Amperes. Blue points are experimental data. Red lines show the best fit by the model with reaction constants reconstructed separately for each experiment.

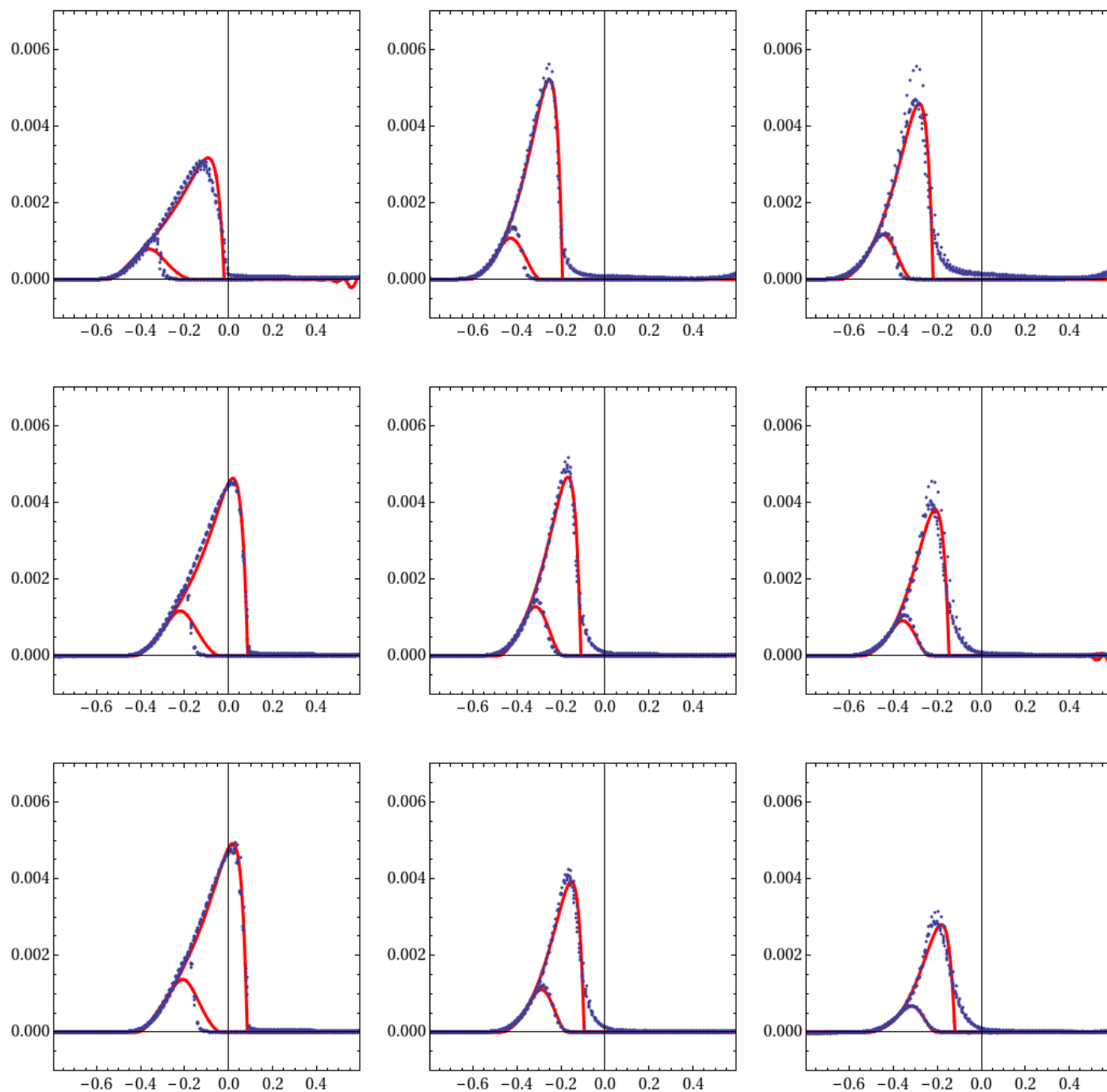


Figure 8. CV experiments. From left to right, the concentration of alkaline KOH is set to $c_1 = \{0.1, 0.5, 1.0\}M$, from bottom to top, the concentration of methanol CH_3OH is set to $c_2 = \{0.5, 0.75, 1.0\}M$. Horizontal axes represent the voltage in Volts, vertical axes – the cell current in Amperes. Blue points are experimental data. Red lines show the best fit by the model with reaction constants reconstructed separately for each experiment.

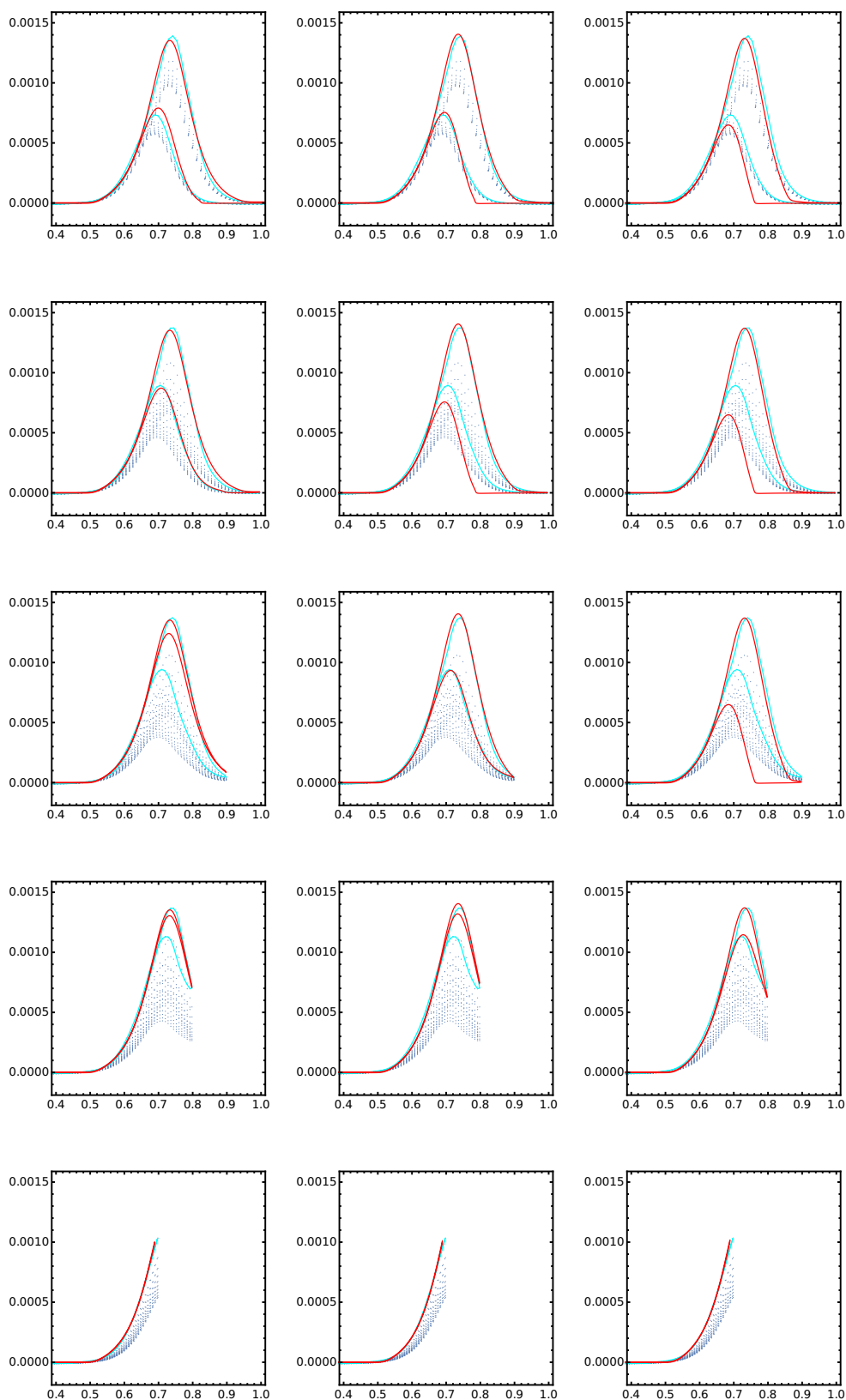


Figure 9. CV experiments, with different upper voltage. Three columns correspond to three isolated optima of the fit. From top to bottom in every column – upper voltage is reduced. Horizontal axes represent the voltage in Volts, vertical axes – the cell current in Amperes. Blue points are experimental data for all cycles. Cyan lines are experimental data for the first cycle. Red lines show the best fit of the first cycle by the model. Data from [12].

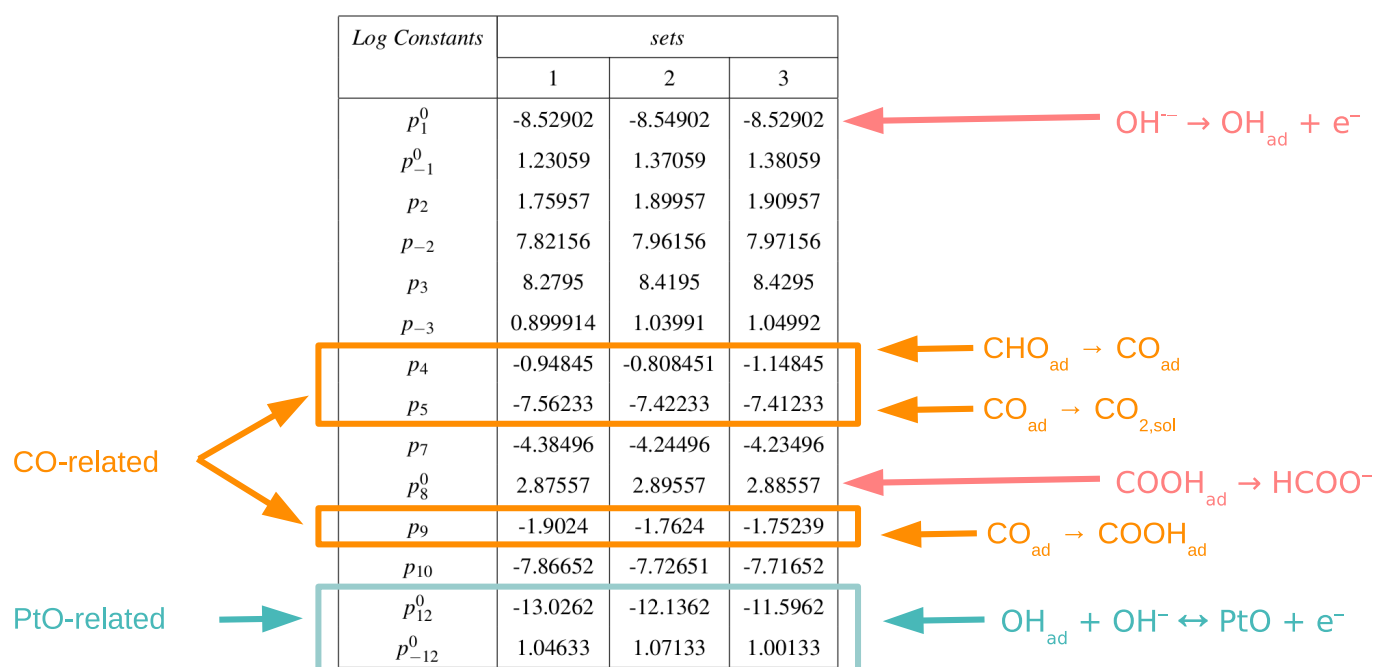


Figure 10. Reconstructed reaction constants for the experiments with different upper voltage. The constants are given in logarithmic values $p_i = \log_{10}(k_i/[\text{mol}/(\text{m}^2\text{s})])$. Two sources of decoupling of reagents (CO-related, PtO-related) are indicated, with corresponding reactions.

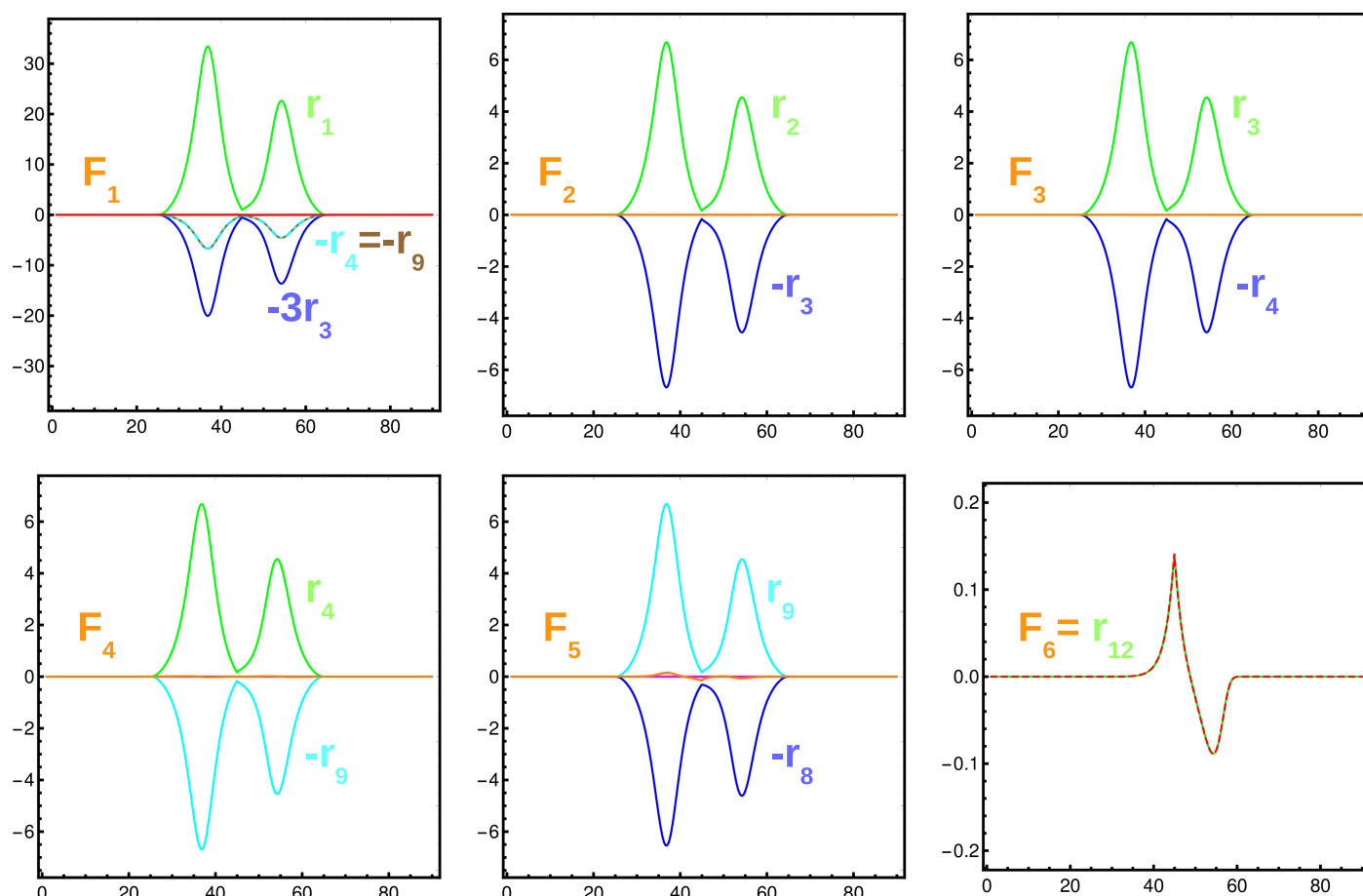


Figure 11. The plots of production rates F_i and reaction rates r_i . All production rates except F_6 show an approach to equilibrium. The horizontal axes show the time in seconds, the vertical axes: F_i and r_i in s^{-1} .

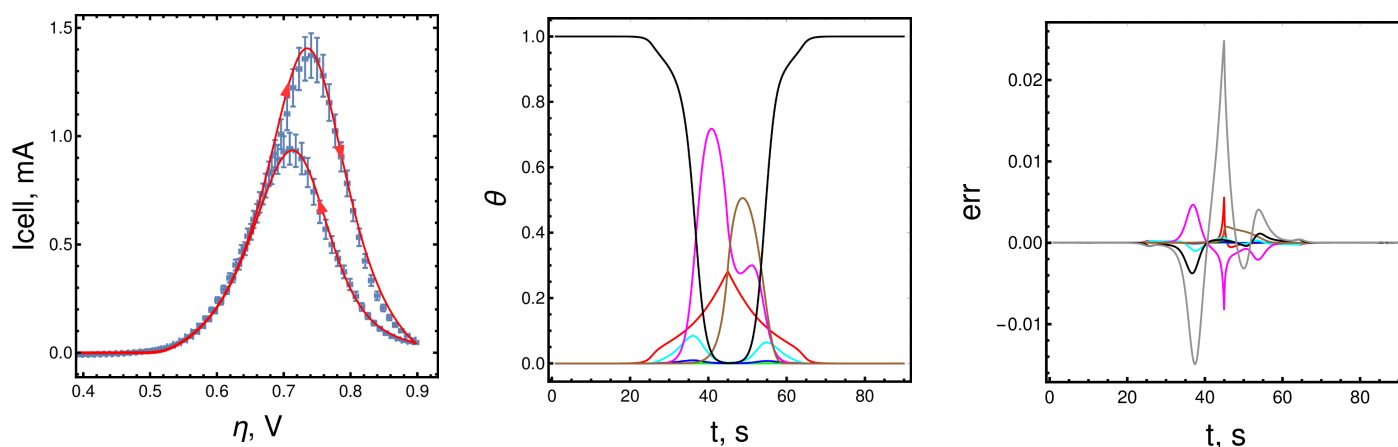


Figure 12. On the left: CV plot, blue points with error bars – the experiment, red line – the model. In the center: evolution of surface coverages, the colors (red, green, blue, cyan, magenta, brown) encode sequential θ_i , black shows the free Pt surface. On the right: ODE \rightarrow DAE variations for θ_i (the same colors), relative variation for I_{cell} (in gray).

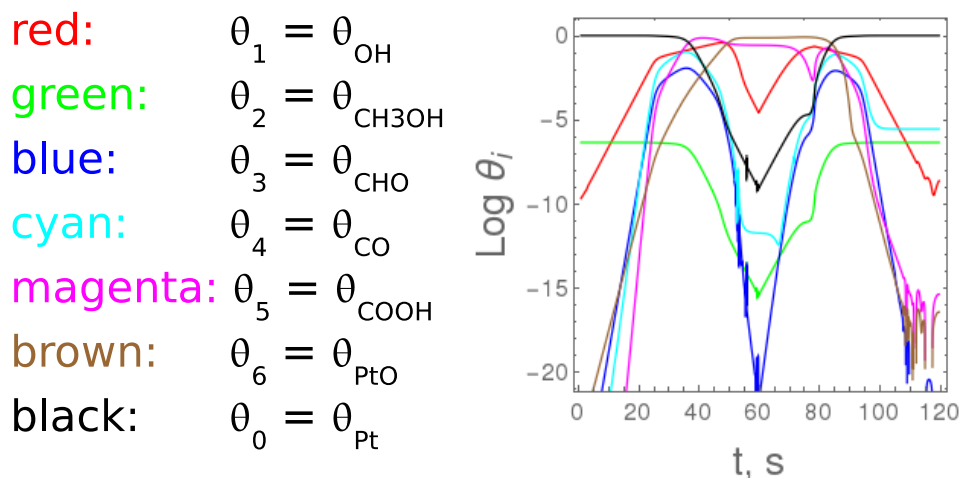


Figure 13. Evolution of θ_i in logarithmic values.

The described mathematical model fits the experimental data well, both for ODE and for DAE formulations, see Figure 12 left. After the transition to DAE, the CV plot in Figure 12 left changes slightly, as well as the detailed evolution of θ_i , shown in Figure 12 center and in logarithmic values in Figure 13. An interesting property that immediately catches the eye is the temporal asymmetry of the profiles for some reagents. Since the voltage is an even periodic function, if all reactions were in equilibrium, all θ_i would be even periodic. They would behave like red or black lines, corresponding to OH_{ad} and free Pt in Figure 12. Deviation from this behavior for magenta and brown, that is, $COOH_{ad}$ and PtO , is a purely dynamic effect. The consequence of this effect is the observed mismatch (hysteresis) for the increasing and decreasing branches of the CV plot. In line with this work, it is important that DAE provides essentially the same profiles as ODE. Figure 12 right measures the deviation between the DAE and ODE, for θ_i , in the same colors, as well as the deviation of I_{cell} relative to its maximum, shown in gray. As a result, the transition from ODE to DAE results in 0.8% maximal variation

for θ_i and 2.5% for I_{cell} , proving a good accuracy of the DAE representation.

V. CONCLUSION

In this paper, alkaline methanol oxidation has been considered, an important electrochemical process in the design of efficient fuel cells. The reaction network, represented as a hypergraph of reactions, connecting multiple reagents, is automatically translated to the mathematical model, including an ODE system describing the kinetics of the process. The difference between the modeled and experimentally measured current of the cell is used for the fitting of the parameters of the underlying mathematical model. Three types of experiments (PC, EIS, CV) can be used for the identification of the parameters.

Further, the model reduction can be performed by setting fast reactions to the equilibrium and leaving the dynamical term only for slow reactions. The obtained DAE formulation has an advantage that only one degree of freedom (surface

coverage by PtO) remains in the system, to which the evolution of other reagents is strictly coupled. The model is reduced and still describes the same effects as the complete system. In particular, it explains the dynamic hysteresis of volt-ampere characteristics of the cell. The methods have been tested on a range of experiments, including different concentrations of the reagents and different voltage range.

VI. ACKNOWLEDGMENT

The work has been partially supported by the German Federal Ministry for Economic Affairs and Energy, grant BMWI-0324019A, project MathEnergy and by the German Bundesland North Rhine-Westphalia, the European Regional Development Fund, grant Nr. EFRE-0800063, project ES-FLEX-INFRA.

REFERENCES

- [1] T. Clees, B. Klaassen, I. Nikitin, L. Nikitina, S. Pott, U. Krewer, and T. Haisch, "Model Reduction in the Design of Alkaline Methanol Fuel Cells", Proc. of INFOCOMP 2019, July 28, 2019 to August 02, 2019 - Nice, France, pp. 21-22, Pub. IARIA 2019, ISBN: 978-1-61208-732-0.
- [2] T. Clees, I. Nikitin, L. Nikitina, S. Pott, U. Krewer, and T. Haisch, "Parameter Identification in Cyclic Voltammetry of Alkaline Methanol Oxidation", in Proc. SIMULTECH 2018, July 29-31, 2018, Porto, Portugal, pp. 279-288, ISBN: 978-989-758-323-0.
- [3] T. Clees, I. Nikitin, L. Nikitina, S. Pott, U. Krewer, and T. Haisch, "Mathematical Modeling of Alkaline Methanol Oxidation for Design of Efficient Fuel Cells", in: Obaidat M., Ören T., Rango F. (eds) Simulation and Modeling Methodologies, Technologies and Applications, SIMULTECH 2018, Advances in Intelligent Systems and Computing, vol 947, 2020 (First Online 20 November 2019), pp. 181-195, Springer, DOI: 10.1007/978-3-030-35944-7_9.
- [4] T. Clees, I. Nikitin, L. Nikitina, D. Steffes-lai, S. Pott, U. Krewer, and T. Windorfer, "Electrochemical Impedance Spectroscopy of Alkaline Methanol Oxidation", in Proc. INFOCOMP 2017, The Seventh International Conference on Advanced Communications and Computation, pp. 46-51, IARIA, 2017.
- [5] U. Krewer, T. Vidakovic-Koch, and L. Rihko-Struckmann, "Electrochemical oxidation of carbon-containing fuels and their dynamics in low-temperature fuel cells", ChemPhysChem, vol. 12, 2011, pp. 2518-2544.
- [6] U. Krewer, M. Christov, T. Vidakovic, and K. Sundmacher, "Impedance spectroscopic analysis of the electrochemical methanol oxidation kinetics", Journal of Electroanalytical Chemistry, vol. 589, 2006, pp. 148-159.
- [7] B. Beden, F. Kardigan, C. Lamy, and J. M. Leger, "Oxidation of methanol on a platinum electrode in alkaline medium: effect of metal ad-atoms on the electrocatalytic activity", J. Electroanalytical Chem., vol. 142, 1982, pp. 171-190.
- [8] F. Ciucci, "Revisiting parameter identification in electrochemical impedance spectroscopy: Weighted least squares and optimal experimental design", Electrochimica Acta, vol. 87, 2013, pp. 532-545.
- [9] A. J. Bard and L. R. Faulkner, Electrochemical Methods: Fundamentals and Applications, Wiley 2000, ISBN: 978-0-471-04372-0.
- [10] A. Baldin et al., "Universal Translation Algorithm for Formulation of Transport Network Problems", in Proc. SIMULTECH 2018, vol. 1, pp. 315-322.
- [11] A. N. Gorban, "Model reduction in chemical dynamics: slow invariant manifolds, singular perturbations, thermodynamic estimates, and analysis of reaction graph", Current Opinion in Chemical Engineering, vol. 21, 2018, pp. 48-59, DOI: 10.1016/j.coche.2018.02.009.
- [12] T. Haisch et al., "The origin of the hysteresis in cyclic voltammetric response of alkaline methanol electrooxidation", submitted to Physical Chemistry Chemical Physics.